THE RESISTIVELY-LOADED V-ANTENNA

CURRENT DISTRIBUTION
IMPEDANCE AND TERMINAL-ZONE CORRECTION
RADIATION FIELD

By

Bob M. Duff

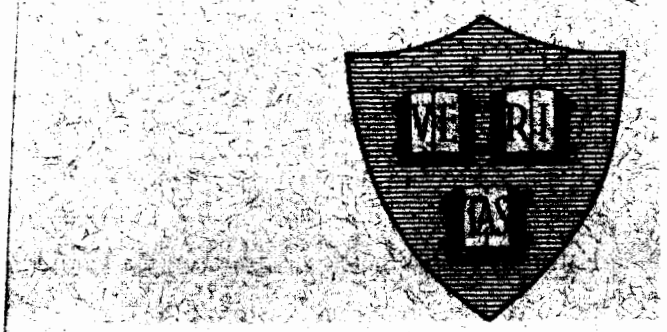

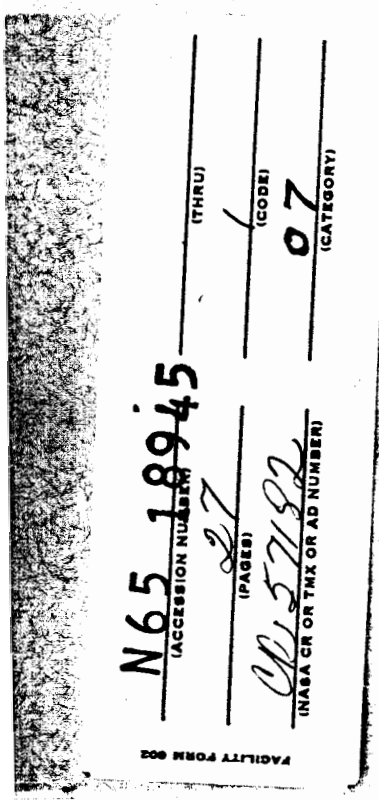

UNPUBLISHED PRELIMINARY DATA

Scientific Report No. 3

October 1964

Prepared under Grant No. NsG 579 at
Gordon McKay Laboratory, Harvard University
Cambridge, Massachusetts
for
NATIONAL AERONAUTICS AND SPACE ADMINISTRATION

THE RESISTIVELY-LOADED V-ANTENNA

CURRENT DISTRIBUTION

IMPEDANCE AND TERMINAL-ZONE CORRECTION

RADIATION FIELD

By Bob M. Duff

Scientific Report No. 3

October 1964

Prepared under Grant No. NsG 579 at
Gordon McKay Laboratory, Harvard University
Cambridge, Massachusetts

for

NATIONAL AERONAUTICS AND SPACE ADMINISTRATION

MEASUREMENT OF THE DISTRIBUTION OF CURRENT ALONG A RESISTIVELY-LOADED V-ANTENNA

By Bob M. Duff

Gordon Mc Kay Laboratory, Harvard University
Cambridge, Massachusetts

SUMMARY

The apparatus used to measure the distribution of current along a V-antenna that is resistively loaded about a quarter wavelength from the end is described. The measured distributions of current for several angles Ψ between the arms of the V are shown graphically for antennas with arm lengths $h = \lambda$ and $h = 2\lambda$. In each case a resonant upper section about $\lambda/4$ in length is connected to the main antenna by means of a resistor R. It is shown that with R near $120(\ln 2h/a - 1)$ ohms the current on the main section is essentially a traveling wave with nearly constant amplitude and uniformly increasing phase. This distribution is affected only slightly by changes in the angle Ψ between the arms of the V. It is changed if R is varied significantly from the above mentioned value.

INTRODUCTION

The directional properties of a V-antenna are enhanced if the current over the greater part of the length is a traveling wave. The work of Altschuler (ref. 4) on a resistively-loaded dipole has shown that, if resistors of proper size are connected in series with the antenna near a quarter wavelength from its ends, the currents in the outer quarter-wave sections are standing waves, and the currents in the main sections are essentially traveling waves. If the dipole is folded to form a V-antenna, similar distributions of current should obtain. In the following, the current distribution along a V-antenna which has each arm resistively loaded near a quarter wavelength from the end is measured. The angle Ψ between the arms of the V, the length h of the arms and the loading resistance R are the parameters.

EXPERIMENTAL EQUIPMENT AND MEASURING TECHNIQUE

The Antenna

For the measurement of the current distribution and input impedance, an image-plane antenna was used. This antenna consisted of one-half of a

traveling-wave V-antenna mounted in front of a vertical image plane. The geometry of the antenna is shown in Fig. 1 and the following notation is used:

$\Psi/2$: Angle between the antenna element and the image screen, or 1/2 of the angle between the elements of the full V-antenna.

h_1 : Length of the traveling-wave portion of the antenna measured from the image plane to the mid-point of the load resistor.

h_2 : Length of the standing-wave portion of the antenna measured from the mid-point of the load resistor to the end of the antenna.

$h = h_1 + h_2$

R : Resistance of the load resistor measured in ohms.

The image plane consisted of a 17 by 20 foot aluminum screen mounted vertically on the side of the building with its center opposite a third-floor window through which connections to the measuring line were made. The antenna itself was constructed of brass tubing 1/4 inch outside diameter. The traveling-wave section of the antenna contained a 1/16 inch slot parallel to its axis through which a current measuring probe could be extended. The two antenna sections were machined so that a resistor could be mounted between them, and the standing-wave section was terminated by a hemispherical end cap. An angle coupling section was used to connect the antenna to the center conductor of the driving line. By using different coupling sections, it was possible to obtain any desired angle between the antenna and the image plane. Ideally, the joint between the antenna and the driving line should lie in the plane of the image screen; however, when using the same diameter for the antenna and center conductor of the line this is impossible. The convention adopted for these measurements was to set the inside edge in line with the image plane, as shown in Fig. 1.

A polyfoam block was used to support the antenna in a horizontal plane in front of the image screen. This support measured 20 x 22 x 140 centimeters and was held in position by nylon cords attached to the top and sides of the image screen. The antenna and polyfoam mount could be positioned at any angle with respect to the image screen, from 10 degrees to 90 degrees.

Most of the measurements which have been made were on an antenna of total length of one wavelength, and at a frequency of 600 Mc./sec.. For this antenna, $\Omega = 2\ \ell n\ (2\ h/a) = 11.5$.

The Measuring Equipment

The antenna described above was driven from a horizontally mounted coaxial line whose outer conductor was connected directly to the image screen, and inner conductor to the antenna. Both the inner conductor of the line and the antenna were slotted to carry a small current measuring probe. The measuring equipment was generally the same as that used for many antenna measurements here and is described completely by Andrews (ref. 1).

The coaxial line was constructed of an outer conductor formed of brass tubing 2.032 inches outside diameter, and an inner conductor of 1/4 inch outside diameter brass tubing. The space between the two conductors was entirely filled with polyfoam. The end of the line away from the image screen is terminated by a non-contacting short circuit. Behind the main line assembly is a long rack and pinion and steel metric scale assembly. The terminating short circuit, the center conductor and the measuring probe can all be positioned by hand wheels, and changes in position measured to about 1/10 mm.

The current measuring probe is a small shielded loop about 1/10 inch in diameter. This type of probe and the effects of the slot on the field distribution have been discussed by Morita (ref. 2). A small coaxial line is used to carry the energy from the probe back through the main coaxial line and to the measuring equipment. This line is also used to hold the probe in position. The end of the probe away from the driving line is connected to a string and weight arrangement which keeps the coaxial line taut at all times, and thus serves to allow accurate positioning of the probe.

The main coaxial line is excited by a transmitter consisting of a high frequency coaxial line oscillator. The transmitter is tunable over a range of 350 - 700 Mc/sec.; however, all measurements have thus far been made at 600 Mc/sec. For detection and measurement of the signal from the probe, a General Radio Unit IF amplifier and local oscillator were used. For measurement of phase a slotted line terminated by a matched load provided a reference signal. This reference signal and the signal from the probe were fed to a hybrid junction and the difference signal was then observed. Figure 2 shows the entire measuring arrangement in block diagram form.

Measurement of the Current Distribution

Current distribution measurements were made along the traveling wave portion of the antenna for various values of the angle $\Psi/2$ and various values of load resistance R . For the full wave antenna $h = \lambda$, measurements have been completed at angles of $\Psi/2 = 10, 20, 35, 45, 60, 70, 83$, and 90 degrees. For the two-wavelength antenna, measurements were made at $\Psi/2 = 45, 60, 70, 83$, and 90 degrees. The primary purpose of these measurements was to

answer two questions: first, what value of load resistance was needed to obtain satisfactory traveling-wave conditions and second, how these conditions vary with the angle.

It should be pointed out that the standing-wave section used was not $\lambda/4$, but rather the resonant length. For a section of about $\lambda/4$ of this antenna, $\Omega = 8.75$. From data tabulated by King (ref. 3), the resonant length is found to be $h = 11.5$ cm. Both a $\lambda/4$ section and the resonant section were tried and a significant improvement in the amount of standing wave was observed when using the resonant length.

As pointed out by Altschuler (ref. 4), a value for R can be predicted from the zero-order expression for the input impedance of a dipole:

$$Z_{IN} = -j \frac{\zeta_o}{2\pi} \Psi \cot \beta_o h \qquad (1)$$

taking the value of R as

$$R = \zeta_o \Psi / 2\pi$$

where

$$\Psi \doteq \Omega - 2 = (2 \ln (2h/a) - 2) .$$

In considering the V-antenna, the variable characteristic impedance as given by Schelknoff (ref. 5) for a section of tapered two-wire line open at $z = h$ and closed at $z = 0$ would seem appropriate:

$$R_c = (\zeta_o/2\pi)\, 2 \ln \left(\frac{2z \sin(\Psi/2)}{a} \right) \qquad (2)$$

It is seen that for the angle $\Psi/2 = 90^\circ$ (dipole case), the two formulas would agree in the limit as Ω becomes very large. Taking $R_c/2$ as the value of load resistance to be used in each half of the antenna, equation 1 gives 285 ohms for a one-wavelength dipole antenna. If equation 2 is used with $\Psi/2 = 90^\circ$ and $z = 3/4\lambda$, a somewhat higher value of 330 ohms is obtained. For $\Psi/2 = 45^\circ$, equation 2 would predict R = 308 ohms, and at $\Psi/2 = 10^\circ$, R = 222 ohms.

The amplitude and phase distribution of current along the traveling-wave portion of the antenna were measured for a number of different values of $\Psi/2$ and in most cases for different values of R. Typical results are shown in Fig. 3. It can be seen that R = 240 ohms produces a good traveling-wave condition in all cases. However, there is an indication that the value of R should be decreased with $\Psi/2$ to obtain the optimum traveling-wave condition as predicted by equation 2.

It should be pointed out that because of restrictions imposed by the size of the probe and the construction of the antenna, the measurements extend only from a point 3.5 cm. from the image plane to a point 3.5 cm. from the load resistor R.

CONCLUSION

It has been verified experimentally that the distribution of current along a resistively-loaded V-antenna of length h and radius a is essentially a traveling wave between the driving point and the loading resistor R provided $R = 2(\ln 2h/a - 1)$ ohms. The resistor must be located near a quarter wavelength from the end. This distribution is affected relatively little by changes in the apex angle Ψ of the V and by the length of the antenna.

REFERENCES

1. H. W. Andrews, "Image-Plane and Coaxial Line Measuring Equipment at 600 Mc.," Cruft Laboratory Technical Report No. 177, Harvard University, July 1, 1953.

2. T. Morita, "The Measurement of Current and Charge Distributions on Cylindrical Antennas," Cruft Laboratory Technical Report No. 66, Harvard University, February 1, 1949.

3. R. W. P. King, The Theory of Linear Antennas, Harvard University Press, p. 168, 1956.

4. E. E. Altschuler, "The Traveling-Wave Linear Antenna," Scientific Report No. 7 (Series 2), AF19(604)-4118, Cruft Laboratory, Harvard University, May 5, 1960.

5. S. Schelkunoff, Electromagnetic Waves, Van Nostrand, New York, 1943.

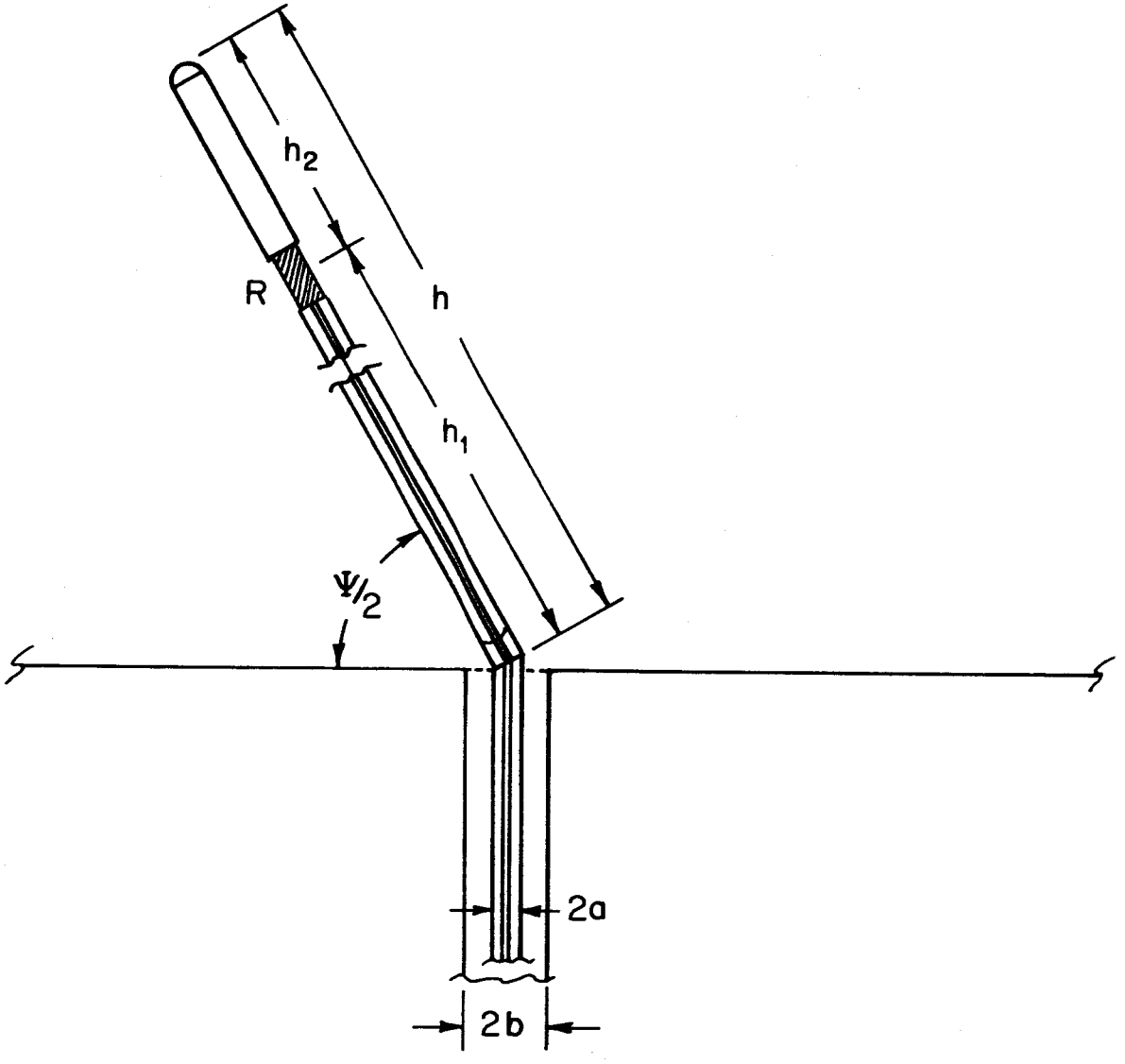

FIG. 1 GEOMETRY FOR THE ANTENNA .

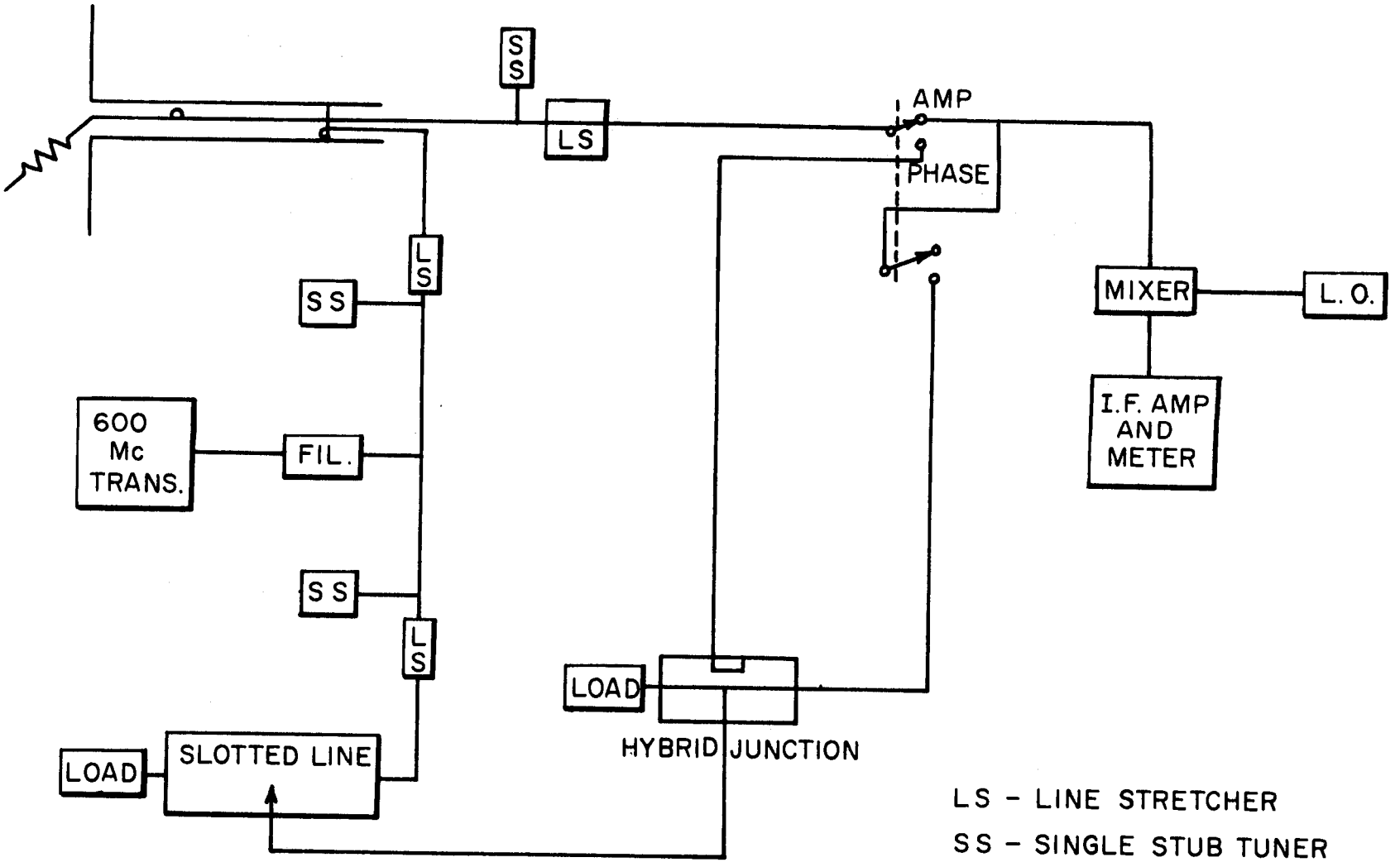

FIG. 2 BLOCK DIAGRAM OF EQUIPMENT

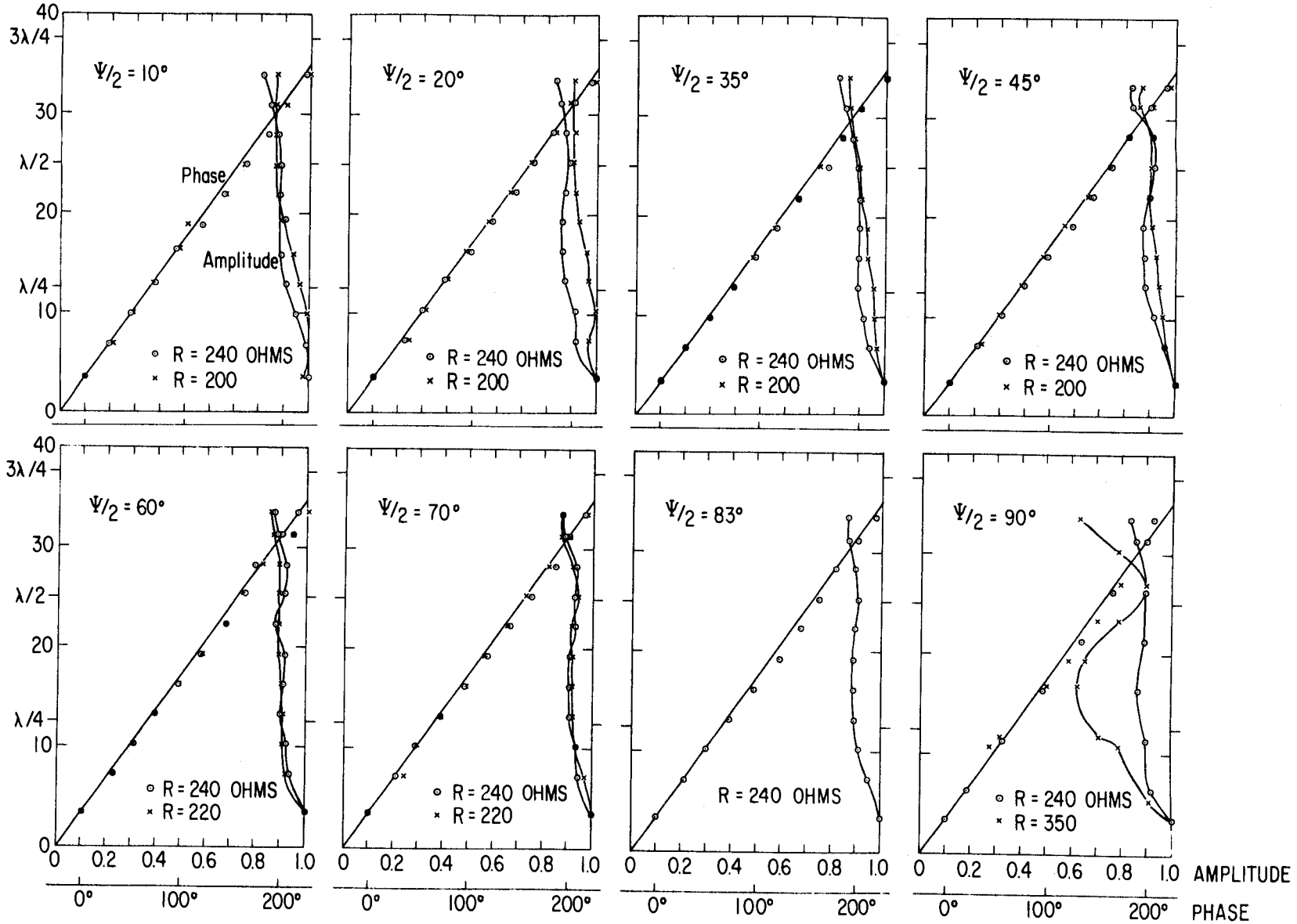

FIG. 3 DISTRIBUTION OF CURRENT ON RESISTIVELY-LOADED V-ANTENNA WITH $h = \lambda$.

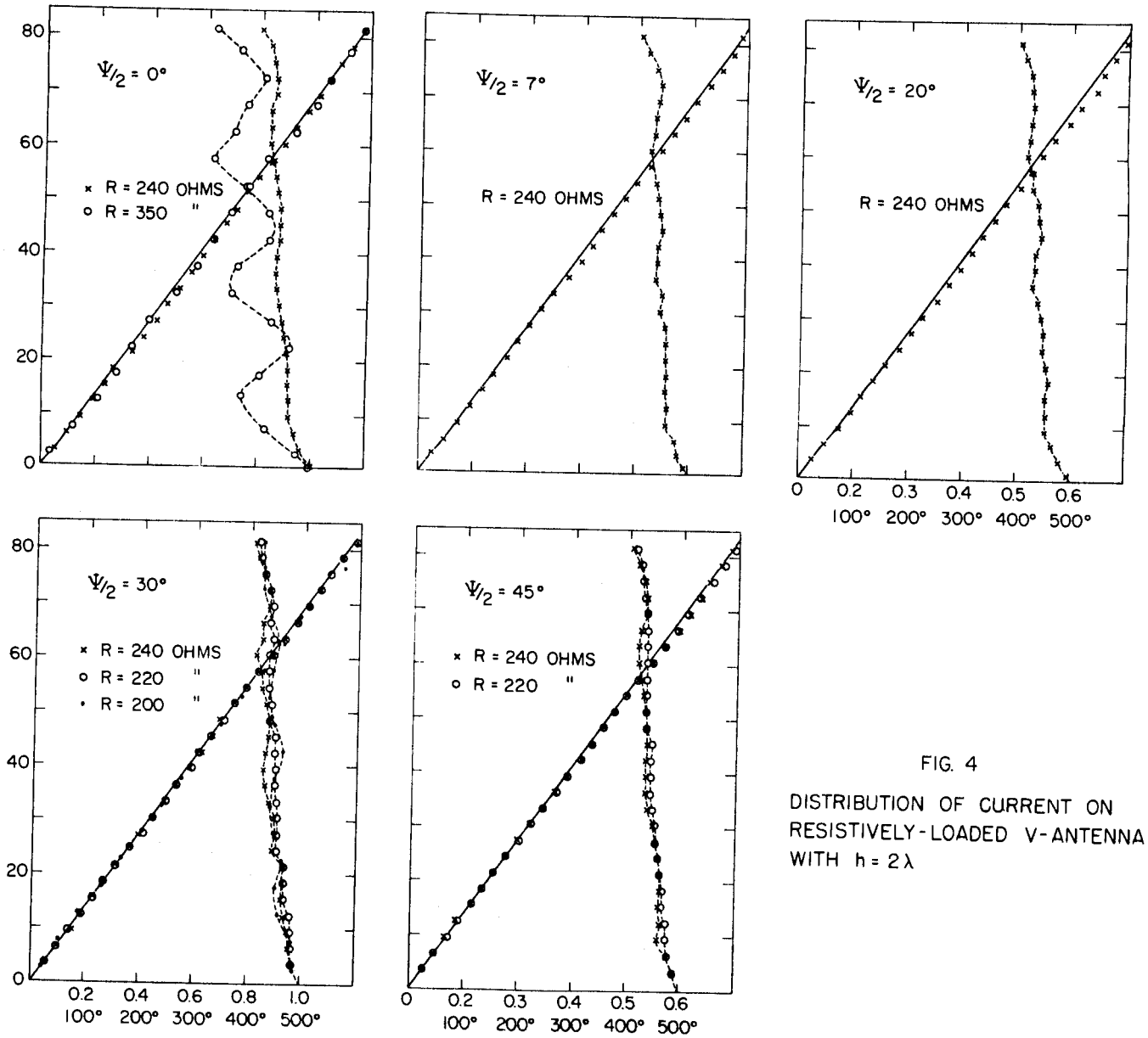

FIG. 4

DISTRIBUTION OF CURRENT ON RESISTIVELY-LOADED V-ANTENNA WITH $h = 2\lambda$

MEASUREMENT OF IMPEDANCE AND TERMINAL-ZONE CORRECTIONS FOR A RESISTIVELY-LOADED V-ANTENNA

By Bob M. Duff

Gordon Mc Kay Laboratory, Harvard University
Cambridge, Massachusetts

SUMMARY

The driving-point impedance and terminal-zone corrections for a resistively-loaded V-antenna have been measured. These measurements were made on an antenna inclined at an angle $\Psi/2$ to an image plane, and driven by a coaxial line with inner conductor radius a and outer conductor radius b. Transmission-line end sections one-half wavelength long provided five different values of outer conductor radius at the driving point. The measured apparent admittance was plotted as a function of the ratio b/a and extrapolated to the value b/a = 1, which corresponds to the admittance B_s of an ideal slice-generator-driven antenna. For all values of $\Psi/2$ it was found that terminal-zone corrections can be represented by a lumped negative capacitance, and that the apparent susceptance can be represented by the formula:

$$B_{sa} = B_s + K \ln (b/a)$$

where B_s and K are functions of Ψ, and K is negative.

INTRODUCTION

Measurements have shown that with a 250 ohm resistive load located approximately one-quarter wavelength from the end of a V-antenna, the current distribution along the antenna up to the resistor is essentially that of a traveling wave. The impedance of this antenna has now been measured with special attention given to terminal-zone corrections. The self-impedance of an antenna can be defined rigorously in only two instances: when the cross-sectional dimensions of the driving transmission line are vanishingly small, or when the case of an idealized antenna driven by a delta-function generator is considered.

When the antenna is connected to a transmission line of finite dimensions, the antenna and transmission line must be considered as an integral system since the dimensions of the line can greatly affect the apparent impedance terminating it. The terminal-zone correction is the difference between the

measured apparent impedance and the impedance of an idealized antenna. It has been shown by King (ref. 1) that the antenna transmission-line system of linear antennas – including the conventional V-antenna – can be approximately represented by an ideal line terminated by the combination of a lumped constant network and the impedance of an idealized antenna. The lumped constant network then constitutes the terminal-zone corrections.

The problem of terminal-zone corrections is insignificant in many antenna systems, particularly those operating at low frequencies where the transmission-line dimensions are negligible compared to the wavelength. In that case the apparent impedance terminating the line is essentially the same as for an idealized antenna. However, when the antenna is scaled down for convenience in making laboratory measurements, it is usually impractical to scale down the transmission line to the same degree. Terminal-zone corrections then may become very significant. To relate the measurements made on the model to the impedance of the actual antenna system, it is necessary to take into account the terminal-zone corrections.

For laboratory measurements on antennas, it is often desirable to use image plane techniques when the symmetry of the antenna permits this to be done. The measurements described in this report were made on an antenna consisting of one-half of a resistively-loaded V-antenna located above an image plane and driven by a coaxial line. The impedance thus measured is one-half the impedance of an equivalent full V-antenna.

EXPERIMENTAL METHOD AND RESULTS

The method used in this experiment was essentially the same as that used by Hartig (ref. 2) for similar measurements on cylindrical antennas. Measurements of the apparent terminating impedance were made for various line spacings characterized by the ratio b/a, where b is the radius of the outer conductor and a is the radius of the inner conductor of the coaxial line at the driving point (Fig. 1).

The measured values were then extrapolated to the value $b/a = 1$, which corresponds to the impedance of an idealized antenna driven by a delta-function generator. In order to obtain the different values of b/a, end sections of line having different outer radii and each one-half wavelength long were used. The discontinuity in outer radius which occurs one-half wavelength from the end corresponds to a shunt capacitance whose value can be determined either theoretically or experimentally. Hartig (ref. 2) found that the measured values of capacitance for discontinuities of this type

agreed very well with theoretical values. For the present work, theoretical values as given by Winnery, Jamieson, and Robbins (ref. 3) were used.

The measuring equipment was essentially the same as that used previously for current-distribution measurements. Described in detail by Andrews (ref. 4), it consists of a vertically-mounted image plane, to the center of which is connected a horizontally-mounted coaxial line. The antenna is an extension of the inner conductor of the line. The outer conductor of the main coaxial line is a brass tube of 2.03 inch inner diameter, and the inner conductor is a 1/4 inch diameter brass tube which is slotted lengthwise. Current-distribution measurements were made with a small loop probe which extended out through the slot in the inner conductor. For measurement of the current distribution of the antenna, the probe had been connected to a rack and pinion by a flexible cable. This cable was replaced by a rigid tube for the impedance measurements in order to improve the accuracy of probe-position measurements. All data in the present work were taken at a frequency of 600 Mc.

The apparent impedance terminating the line was determined by means of a distribution-curve method. For each measurement the mean value of at least three mid-point determinations at each of at least three current minima was used.

Most of the data were taken on an antenna of total length of 75 cm. Additional data have been obtained for the lengths 25, 50, 100, 125, and 150 cm.; however, these are not sufficiently complete for the determination of the exact dependence of the apparent impedance on length. The data presently available indicate that from 50 to 150 cm. length the impedance differs very little from that of the 75 cm. length. The 25 cm. antenna, however, showed a significant decrease in impedance.

The apparent admittance terminating the line was measured using the 75 cm. antenna for values of b/a equal to 8.12, 7, 6, 4, and 2; and for angles of 10, 20, 35, 45, 60, 70, 83, and 90 degrees. The results are shown in Table I. The conductance G_{sa} fluctuates slightly with b/a, although no definite pattern could be found. It was concluded that, within the accuracy of this experiment, G_{sa} is independent of b/a, and the mean value of G_{sa} for each angle was taken as G_s.

With this assumption it is possible to express the apparent susceptance as: $B_{sa} = B_s + B_t$, where B_s is the susceptance of an idealized antenna and B_t is the shunt susceptance of the terminal-zone-correction network. The measured values of B_{sa} are plotted in Fig. 2 as functions of b/a with $\Psi/2$ as a parameter. From these figures it can be seen that B_{sa} can be well represented by the relation:

$$B_{sa} = B_s + K \ln (b/a)$$

where B_s and K are functions of $\Psi/2$, and K is negative. The value of B_s was obtained by extending the curves in Fig. 2 to the value b/a = 1. The difference between B_{sa} and B_s then gives B_t. The values thus obtained for B_t are plotted in Fig. 3, and from this it can be seen that B_t is essentially proportional to $\ln(b/a)$. The values obtained for B_s, G_s, and K are shown in Fig. 4 as functions of $\Psi/2$. R_s and X_s were computed from Y_s and are plotted in Fig. 5. It should be noted that in this arrangement the antenna would be in contact with the image plane for $\Psi = 0$; hence, the impedance must approach zero as Ψ does.

Although much work remains to be done for a complete description of the impedance of this antenna as a function of length, frequency, etc., the data presented here should serve as a basis for comparison with theoretical analysis and as a practical tool in determining the measured apparent impedance of similar antennas when driven from a coaxial line.

CONCLUSION

The fact that the data presented here were obtained from an image-plane antenna driven by a coaxial line may seem to limit their usefulness in application to full V-antennas driven in a quite different manner. However, the impedance determined here can be applied to any resistively-loaded V-antenna for which the dimensions of the transmission line – and hence, the terminal-zone corrections – are negligible.

Since the impedance of a full V-antenna is twice that of the image-plane antenna, the terminal-zone corrections determined here may be applied also to a larger class of antenna installation. For example, consider the case of a resistively-loaded V-antenna which consists of two elements protruding from a conducting surface of essentially arbitrary shape. Each element is connected to a coaxial line whose outer conductor is connected to the conducting surface. If the surface on which the antenna is mounted is small with respect to a wavelength, the impedance of the antenna will be essentially that of an isolated full V-antenna.

On the other hand, terminal-zone effects are essentially local in nature, since they are determined by a region whose dimensions are a few multiples of the outer diameter of the coaxial line. Therefore, if the driving points of the two elements are separated by a large distance as compared to the diameter of the coaxial line, and the surface is basically plane over a small area around each element, then each element appears as an image-plane antenna as far as terminal-zone corrections are concerned. In that case, the data presented in this report are applicable.

In this type of installation, it is likely that each element will produce an angle of nearly 90° with respect to the conducting surface, and it is this angle – rather than the angle between elements of the V – which determines the terminal-zone corrections. In this connection it may be noted that the factor K is a slowly varying function of $\Psi/2$ for $\Psi/2$ near 90°, as can be seen in Fig. 5. For most applications, K can be considered as constant for angles greater than about 45°.

REFERENCES

1. R. W. P. King, The Theory of Linear Antennas, Harvard University Press, 1956.

2. E. O. Hartig, "Circular Apertures and Their Effects on Half-Dipole Impedances," Harvard University Doctoral Dissertation, 1950.

3. J. R. Winnery, H. W. Jamieson, and T. E. Robbins, "Coaxial-Line Discontinuities," Proceedings IRE, p. 695, November 1944.

4. H. W. Andrews, "Image-Plane and Coaxial-Line Measuring Equipment at 600 Mc.," Cruft Laboratory Technical Report No. 66, Harvard University, July 1953.

TABLE 1

Y_{sa} in millimhos

$\Psi/2$	(b/a) = 8.12	7	6	4	2
10	10.92 + j1.78	11.10 + j2.07	11.18 + j2.92	10.92 + j4.10	10.6 + j5.88
20	8.56 + j2.10	8.58 + j2.26	8.75 + j2.56	8.58 + j3.54	8.50 + j4.83
35	7.08 + j1.98	6.92 + j2.07	7.05 + j2.24	7.05 + j2.78	7.08 + j3.94
45	6.47 + j1.78	6.47 + j1.95	6.47 + j2.19	6.60 + j2.64	6.67 + j3.66
60		6.20 + j1.83		6.24 + j2.52	6.27 + j3.41
70	5.90 + j1.70	6.04 + j1.83	5.99 + j1.99	5.99 + j2.48	6.03 + j3.12
83		5.90 + j1.75		6.03 + j2.32	6.10 + j3.20
90		5.99 + j1.79		6.10 + j2.32	6.20 + j3.08

TABLE 2

$\Psi/2$	Y_s millimhos	Z_s ohms	K
10	10.9 + j7.6	61 - j43	-2.735
20	8.6 + j6.2	76 - j55	-2.02
35	7.0 + j5.0	94 - j66	-1.56
45	6.5 + j4.6	102 - j71	-1.34
60	6.2 + j4.3	109 - j74	-1.26
70	6.0 + j3.8	118 - j75	-1.01
83	6.0 + j4.0	114 - j77	-1.17
90	6.0 + j3.8	118 - j74	-1.04

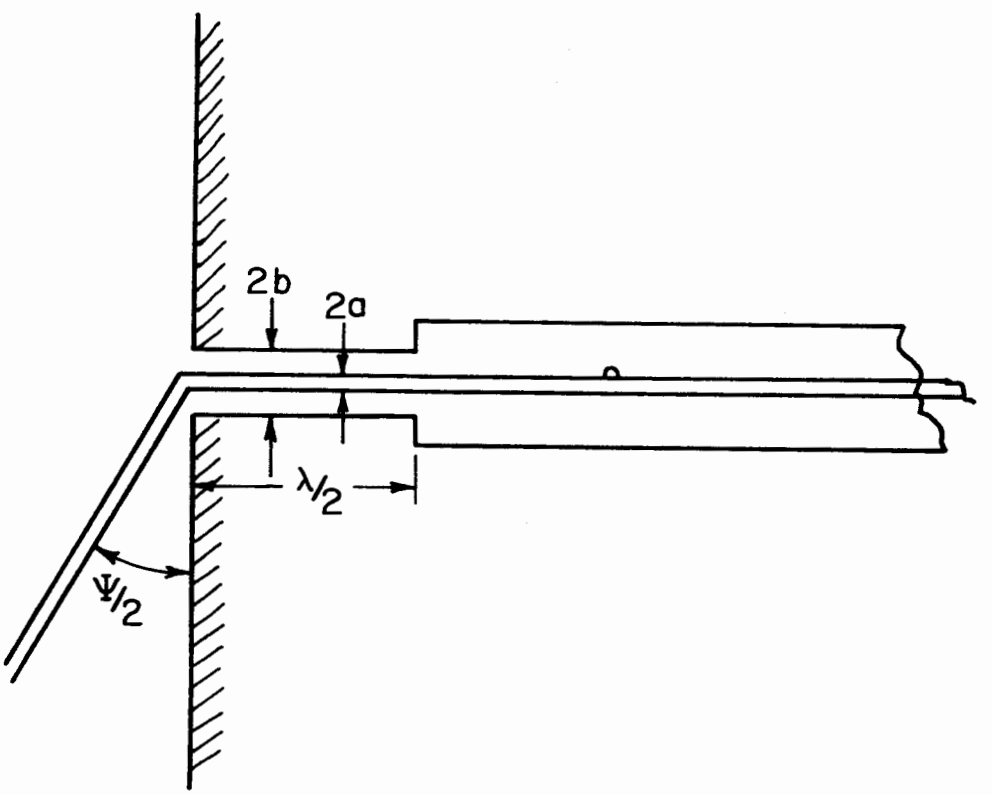

FIG. 1 GEOMETRY FOR THE ANTENNA

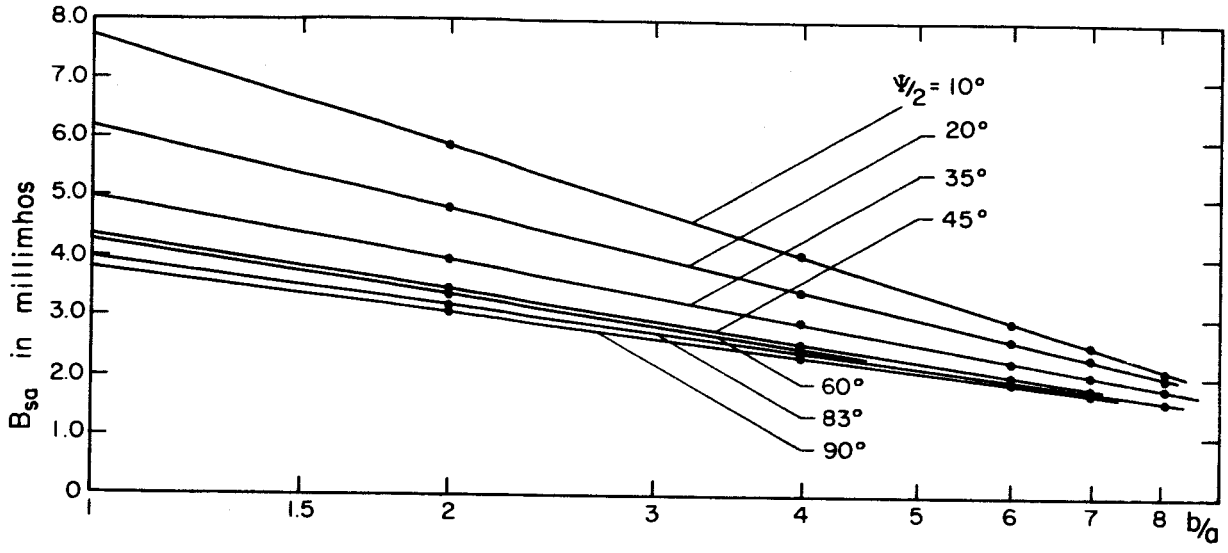

FIG. 2 MEASURED APPARENT SUSCEPTANCE $B_{sa} = B_s + B_t$

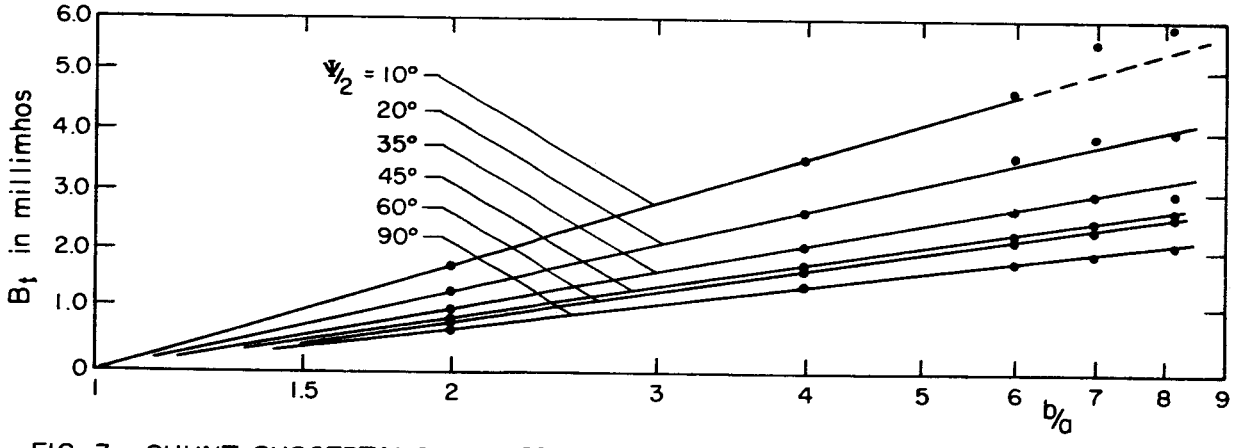

FIG. 3 SHUNT SUSCEPTANCE B_t OF THE TERMINAL-ZONE-CORRECTION NETWORK

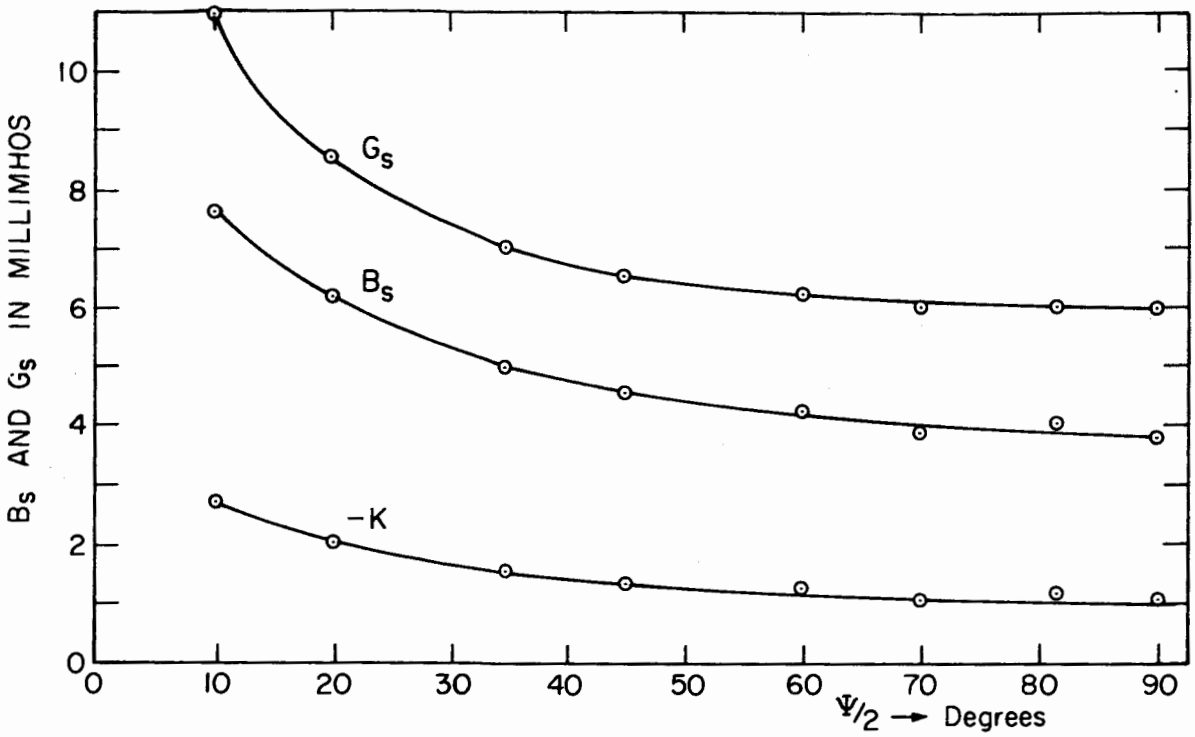

FIG. 4 SUSCEPTANCE B_s, CONDUCTANCE G_s AND K AS FUNCTIONS OF $\Psi/2$; APPARENT SUSCEPTANCE $B_{sa} = B_s + K \ln b/a$.

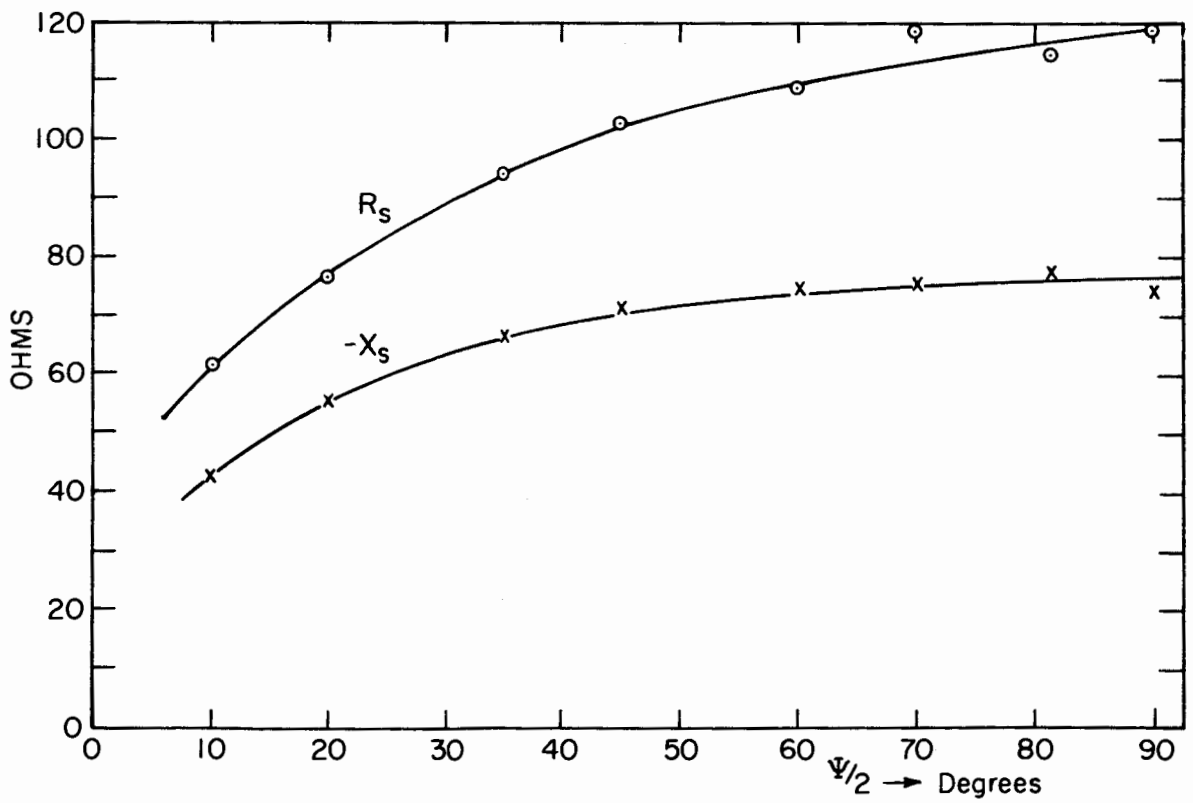

FIG. 5 RESISTANCE R_s AND REACTANCE X_s AS A FUNCTION OF $\Psi/2$.

THE RADIATION FIELD OF A RESISTIVELY-LOADED V-ANTENNA

By Bob M. Duff

Gordon McKay Laboratory, Harvard University
Cambridge, Massachusetts

SUMMARY

Theoretical formulas for the far field of a traveling-wave V-antenna are derived under the assumption that the current between the load resistors is a traveling wave, the current in the quarter-wave end sections outside the load resistors is a standing wave. Graphs of field patterns for an antenna with arm length $h = \lambda$ are displayed for several apex angles Ψ of the V.

ASSUMED CURRENT DISTRIBUTION

The radiation field pattern of a traveling-wave V-antenna can be computed if the distribution of current is known. For purposes of obtaining a preliminary evaluation of the field pattern, it is assumed that a pure traveling wave exists up to the resistive load and a sinusoidal standing wave from the load to the end. Furthermore, the current is assumed to be continuous at the load resistor. These assumptions are reasonable approximations of the measured currents. Let

$$I = I_m e^{-(\alpha+j\beta_o)x} \qquad 0 \leq x \leq h_1 \tag{1}$$

$$I = I_m' \sin \beta_o [(h_1 + h_2)-x] \qquad h_1 \leq x \leq (h_1 + h_2) \tag{2}$$

at $x = h_1$

$$I_m e^{-(\alpha+j\beta_o)h_1} = I_m' \sin \beta_o h_2 \ . \tag{3}$$

It will be assumed in this analysis that $\beta_o h_2 = \pi/2$ so that

$$I_m' = I_m e^{-(\alpha+j\beta_o)h_1} \ . \tag{4}$$

FAR FIELD OF ONE ARM OF THE V-ANTENNA

To obtain the far-zone electric field of the antenna, each element will be considered separately and the results then combined to form the total field of the full antenna. The geometry considered is shown in Fig. 1. For an element lying along the x axis from $x = 0$ to $x = h_1 + h_2$, the far-zone electric field is

$$E_\theta^r = j \frac{\omega}{4\pi \nu_o} \frac{e^{-j\beta_o R_o}}{R_o} \left\{ \int_o^{h_1} I_m e^{-(\alpha+j\beta_o)x} e^{j\beta_o x \cos\theta} \sin\theta \, dx \right.$$

$$\left. + \int_{h_1}^{h_1+h_2} I_m' \sin\beta_o[h_1 + h_2 - x] e^{j\beta_o x \cos\theta} \sin\theta \, dx \right\} \tag{5}$$

Substituting the value of I_m' in terms of I_m

$$E_\theta^r = \frac{j\omega}{4\pi \nu_o} \frac{e^{-j\beta_o R_o}}{R_o} I_m \sin\theta \left\{ \int_o^{h_1} e^{-(\alpha+j\beta_o)x} e^{j\beta_o x \cos\theta} dx \right.$$

$$\left. + \frac{1}{2j} \int_{h_1}^{h_1+h_2} e^{-(\alpha+j\beta_o)h_1} \left[e^{j[(h_1+h_2)-x]\beta_o} - e^{-j[(h_1+h_2)-x]\beta_o} \right] e^{i\beta_o x \cos\theta} dx \right\} \tag{6}$$

where it is assumed that $\sin\theta$ is constant over the range of integration in so far as amplitude effects are concerned. These integrals can be evaluated directly, and after considerable algebraic manipulation can be expressed as follows:

$$E_\theta^r = \frac{E_o}{\beta_o} \sin\theta \left\{ \frac{\beta_o[\alpha - j(1-\cos\theta)\beta_o]}{\alpha^2 + (1-\cos\theta)^2 \beta_o^2} + e^{-\alpha h_1} \left(\left[\cos\{\beta_o h_1(1-\cos\theta) - j\sin\}\beta_o h_1(1-\cos\theta) \right] \right.\right.$$

$$\left.\left. \left[\frac{-\beta_o[\alpha - j(1-\cos\theta)\beta_o]}{\alpha^2 + (1-\cos\theta)^2 \beta_o^2} + \frac{1}{\sin\theta} \left(F(\theta, \beta_o h_2) + j W(\theta, \beta_o h_2) \right) \right] \right) \right\} \tag{7}$$

where

$$E_o = j \frac{\omega}{4\pi \nu_o} \frac{e^{-j\beta_o R_o}}{R_o} I_m \tag{8}$$

$$F(\theta, \beta_o h_2) = \frac{\cos(\beta_o h_2 \cos\theta) - \cos(\beta_o h_2)}{\sin\theta} \tag{9a}$$

$$W(\theta, \beta_o h_2) = \frac{\sin(\beta_o h_2 \cos\theta) - \cos(\theta)\sin(\beta_o h_2)}{\sin\theta} \tag{9b}$$

for $\beta_o h_2 = \pi/2$

$$F(\theta, \pi/2) = \frac{\cos(\frac{\pi}{2}\cos\theta)}{\sin\theta} \tag{10a}$$

$$W(\theta, \pi/2) = \frac{\sin(\frac{\pi}{2}\cos\theta) - \cos\theta}{\sin\theta}. \tag{10b}$$

In the ideal case of no attenuation for which $\alpha = 0$, and after the separation of the real and imaginary parts, (7) becomes:

$$E_\theta^r = \frac{E_o}{\beta_o}\left\{\cos[\beta_o h_1(1-\cos\theta)]F(\theta,\pi/2) + \sin[\beta_o h_1(1-\cos\theta)]\left[\frac{\sin\theta}{1-\cos\theta} - W(\theta,\pi/2)\right]\right.$$
$$+ j\left[\cos[\beta_o h_1(1-\cos\theta)]\left(\frac{\sin\theta}{1-\cos\theta} + W(\theta,\pi/2)\right) - \sin[\beta_o h_1(1-\cos\theta)]F(\theta,\pi/2)\right.$$
$$\left.\left. - \frac{\sin\theta}{1-\cos\theta}\right]\right\} \tag{11}$$

For an antenna one wavelength long $(h_1 + h_2) = \lambda$, the quantity $\frac{\beta_o E_\theta^r}{E_o}$ has been computed and is given in Table 1.

FAR FIELD OF THE V-ANTENNA

Equation (11) can now be applied to each half of the V-antenna by a suitable interpretation of the angle θ and the observation that $I_{mb} = -I_{ma}$ where a and b designate the halves of the antenna.

To obtain the electric field at an arbitrary point in space, the electric fields due to the currents in the halves of the antenna must be added vectorially. At any point the electric vectors $E_{\theta a}^{r}$ and $E_{\theta b}^{r}$ are perpendicular to R_o (the radius vector), and tangent to great circles in the direction of θ_a and θ_b, respectively.

For points in the plane of the V, $E_{\theta a}^{r}$ and $E_{\theta b}^{r}$ are parallel and can be added directly. With reference to Fig. 1 it is seen that:

$$\begin{aligned} \theta_a &= \theta + \Psi/2 \\ \theta_b &= \theta - \Psi/2 \end{aligned} \tag{12}$$

With these conversion formulas the values of E_{θ}^{r} given in Table 1 can be used to compute the horizontal field pattern for any angle Ψ between halves of the V. Computations were made for $\Psi = 30$, 50, 70, and 90°, and the results are plotted in Fig. 2.

The field pattern in the plane perpendicular to the plane of the V and bisecting the angle Ψ is characterized by the fact that $E_{\theta a}^{r}$ and $E_{\theta b}^{r}$ are equal in magnitude. Their resultant is given by:

$$E^{r} = 2\, E_{\theta a}^{r} \sin(\rho/2) \tag{13}$$

where

$$\sin(\rho/2) = \frac{\sin(\Psi/2)}{\sin\theta_a} \quad ; \quad \cos\theta_a = \cos(\Psi/2)\cos\theta \tag{14a}$$

$$\sin(\rho/2) = \frac{\sin(\Psi/2)}{\sqrt{1-\cos^2\theta\cos^2(\Psi/2)}} \tag{14b}$$

These patterns are also shown in Fig. 2.

It should be noted that these field patterns assume a pure traveling-wave from $0 \leq z \leq h_1$, and that there is no attenuation, $\alpha = 0$. The effect of attenuation could become significant, particularly for very long antennas.

TABLE 1

FAR-ZONE ELECTRIC FIELD OF ONE HALF OF TRAVELING-WAVE V-ANTENNA

θ	Re E	Im E
0	0.0000	0.0000
10	0.9514	-0.0320
20	1.8107	-1.1546
30	2.4105	-0.7878
40	2.4730	-1.8915
50	1.7882	-3.1085
60	0.4780	-3.7034
70	-0.8611	-3.0738
80	-1.4622	-1.4622
90	-1.0000	0.0000
100	0.0747	0.3659
110	0.9497	-0.2198
120	1.1550	-0.9155
130	0.8058	-1.1047
140	0.3041	-0.9109
150	-0.0481	-0.5514
160	-0.1666	-0.2574
170	-0.1278	-0.1020
180	0.0000	0.0000

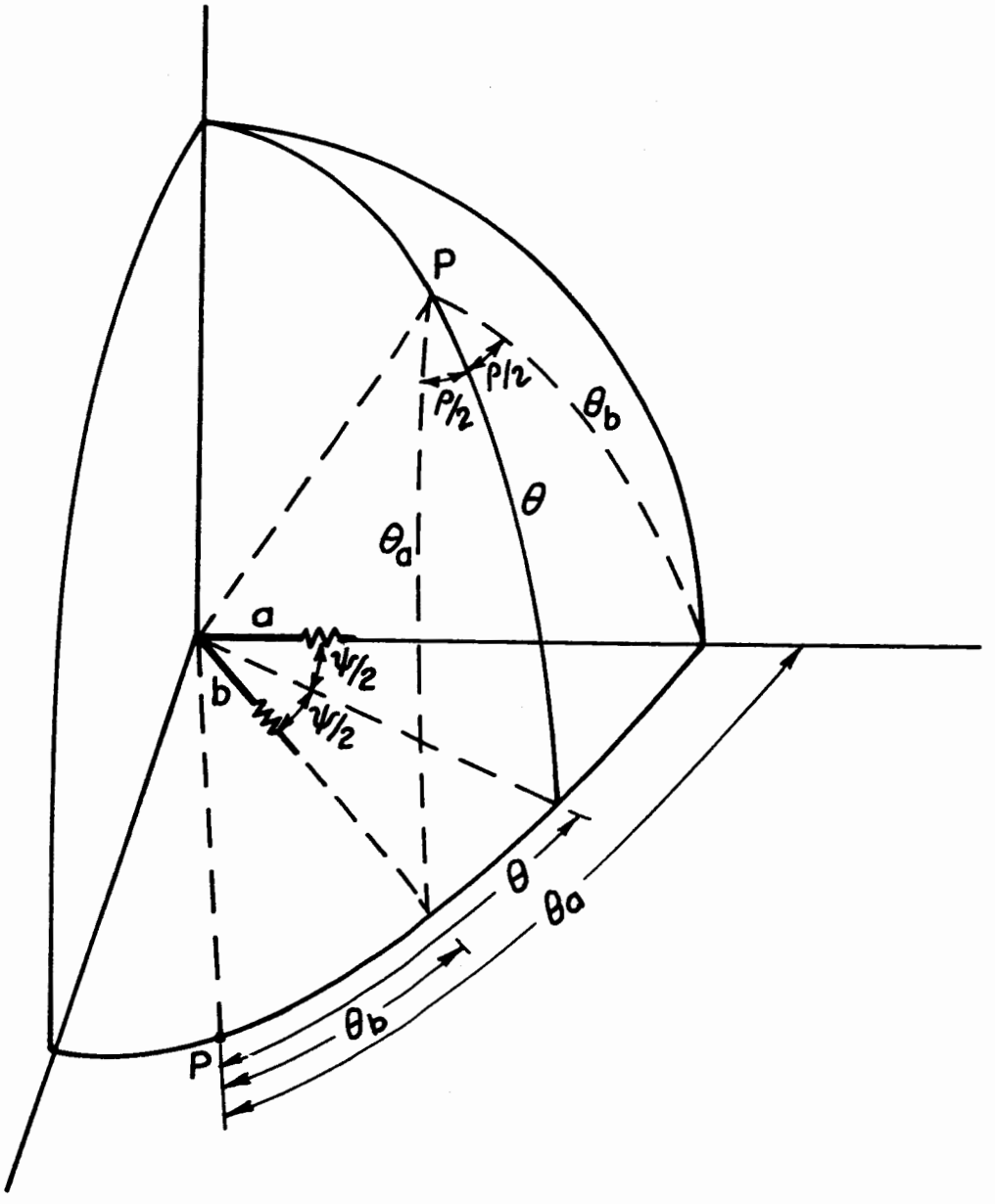

FIG. 1 GEOMETRY FOR THE V-ANTENNA .

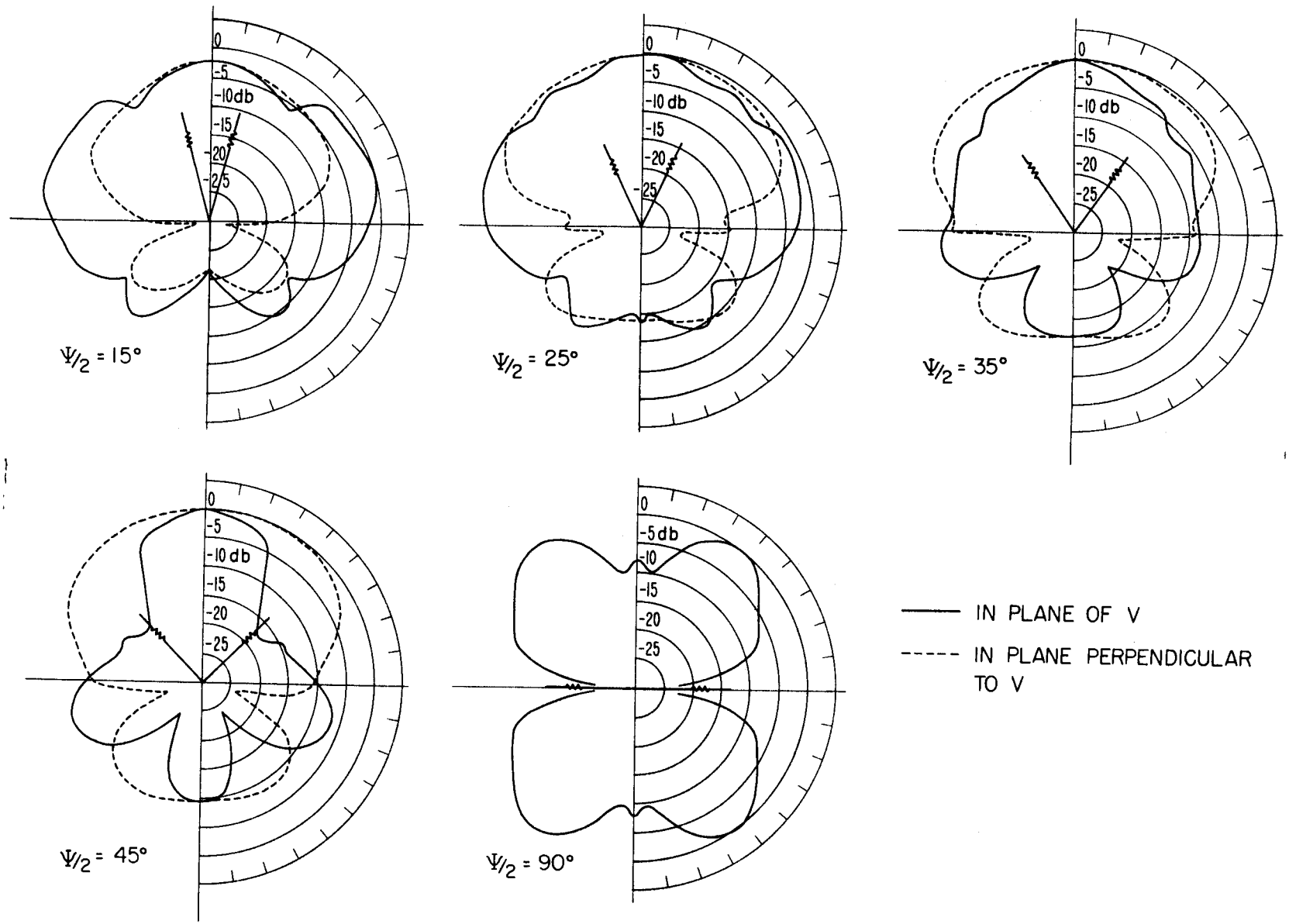

FIG. 2 FAR FIELD PATTERNS OF THE TRAVELING-WAVE V-ANTENNA WITH $h = \lambda$.